

# Removal of cationic and anionic dyes using purified and surfactant-modified Tunisian clays: Kinetic, isotherm, thermodynamic and adsorption-mechanism studies

S. GAMOUDI\* AND E. SRASRA

*Laboratoire de Matériaux Composites et Minéraux Argileux, Centre National des Recherches en Sciences des Matériaux, Technopole de Borj Cedria, Tunisia*

*(Received 27 July 2017; revised 8 December 2017; Guest Associate Editor: Claudio Cameselle)*

**ABSTRACT:** Purified and surfactant-modified Tunisian clays were investigated for their capacity to remove cationic and anionic dyes (crystal violet, CV and methyl orange, MO) from aqueous solution. The samples were characterized by X-ray diffraction (XRD), Fourier transform infrared spectroscopy (FTIR), and potentiometric acid-base titration. Batch-sorption experiments were carried out to evaluate the influence of pH, contact time, initial dye concentration and temperature on the adsorption of dyes. Pseudo-first order, pseudo-second order, intra-particle diffusion and Elovich kinetic models were considered to evaluate the kinetic parameters. To understand the interaction of the dye with the adsorbent, Langmuir, Freundlich, Temkin and Dubinin-Radushkevich isotherms were applied. Thermodynamics studies were conducted to calculate the changes in free energy ( $\Delta^{\circ}G$ ), enthalpy ( $\Delta^{\circ}H$ ) and entropy ( $\Delta^{\circ}S$ ). A difference in the maximum adsorption capacity was observed, suggesting that the retention of dyes was influenced by structure, functional groups of dyes and surface properties of the adsorbents. Moreover, different mechanisms may control the removal of dyes. The purified Tunisian clays are excellent adsorbents for removal of the cationic dye CV and its modified form is suitable for removal of the anionic dye, MO, from aqueous solution.

**KEYWORDS:** dyes, Tunisian clay, adsorption kinetics, equilibrium isotherms, thermodynamics studies.

Dyes are an important class of synthetic organic compounds used in printing, dyeing, textile, food, cosmetics colouring, leather and paper industries. More than 100,000 commercially available dyes exist with  $>8 \times 10^5$ – $10^6$  tonnes produced annually. These compounds have very complex structures, are resistant

to aerobic digestion and are stable to light, heat and oxidizing agents. Indeed, their presence influences water quality because many dyes and their metabolites have been reported to be toxic, carcinogenic and mutagenic (Tang *et al.*, 2014). Very small quantities of dyes can impart colour to large water bodies and make them aesthetically unacceptable, even if they may not be toxic (Sarma *et al.*, 2016). Thus, it is important to treat dye wastes before discharging them into the environment.

The conventional methods for dye removal from contaminated water involve processes such as flocculation (Kono & Kusumoto, 2015), ozonation (Hu

This paper was presented during session: 'ES-02 Environmental applications of clay minerals' at the International Clay Conference 2017.

\*E-mail: [safagamoudi@gmail.com](mailto:safagamoudi@gmail.com)  
<https://doi.org/10.1180/clm.2018.11>

*et al.*, 2016), membrane filtration (Liu *et al.*, 2017), coagulation/flocculation (Yeap *et al.*, 2014), oxidation (Rodrigues *et al.*, 2017), electrochemical or photochemical degradation (Vasconcelos *et al.*, 2015; Guz *et al.*, 2014), photocatalytic or biological degradation (Abdel Messih *et al.*, 2017; Esteves *et al.*, 2016) and adsorption. Among the proposed treatment methods, adsorption technologies are considered to be very viable due to their potential low cost, efficiency and simplicity of design and operation (Gupta *et al.*, 2009). Several adsorbents have been tested to remove synthetic dyes such as activated carbon (Mokhtari *et al.*, 2016; Pelaez-Cid *et al.*, 2016), hydrotalcites (Deng *et al.*, 2016; Bouraada *et al.*, 2016), nanocomposites (Arshadi *et al.*, 2016; Gholami *et al.*, 2016; Hassanzadeh-Tabrizi *et al.*, 2016), hydroxides (Ling *et al.*, 2016; Ruan *et al.*, 2016), and other low-cost adsorbents, in particular, clay minerals (Errais *et al.*, 2012; Leodopoulos *et al.*, 2012; Li *et al.*, 2016b). Among the clay minerals, montmorillonite is considered to be the most suitable adsorbent and it is used widely in dye removal due to its availability, non-toxicity, large specific surface area, high swelling capacity, high cation exchange capacity (CEC) and the presence of several types of active sites on its surface. Untreated and modified montmorillonite have been used successfully as adsorbents for various dyes such as Congo Red (Vimonses, 2009), Acid Orange 7 and Acid Blue 9 (Gil *et al.*, 2011), Malachite Green (Tahir *et al.*, 2010), Acid Blue193 (Özcan *et al.*, 2005) and Basic Red 18 (Ho *et al.*, 2001).

The purpose of the present study was to evaluate the adsorption capacity of purified and surfactant-modified Tunisian clay for anionic and cationic dyes. For this reason, two typical dyes were used: MO (an anionic dye) and CV (a cationic dye). MO is a pH indicator and an industrial dye; it is commonly present in effluent discharges from textile, food, pharmaceutical, printing and paper-manufacturing industries. CV dye, which belongs to the triphenylmethane group, is used widely as an animal medicine in veterinary practice. It is also used for the dyeing of wool, silk, cotton, nylon, paper, leather, *etc.*

In the present study, the samples were characterized by XRD, FTIR and potentiometric acid-base titration. The effects of pH, contact time, initial dye concentration, and temperature were investigated in detail in batch experiments. Another objective of this study was to test various kinetics and equilibrium-isotherm models because a proper mathematical equation represents the relationship between equilibrium adsorption capacity and adsorbate concentration.

## MATERIALS AND METHODS

### Chemicals and materials

The surfactant salt used was hexadecylpyridinium bromide (95% purity), which is a cationic surfactant ( $C_{21}H_{38}N.Br$ ), with molar mass of  $384.44 \text{ g}\cdot\text{mol}^{-1}$  (Sigma Aldrich, St. Louis, Missouri, USA). The cationic dye, CV, and anionic dye, MO, were purchased from Sigma Aldrich (Steinheim, Germany). Some physicochemical characteristics of the dyes used are listed in Table 1. All the reagents were used as received.

The  $Na^+$ -exchanged clay (EP-Na) used in the present study was prepared according to the classical method of Van Olphen (1963). The  $<2 \mu\text{m}$  size fraction was separated by sedimentation in deionized water and was stirred for 24 h with NaCl (1 M). The clay consists of interstratified illite-smectite (I-S) with 78% smectite layers according to Reynolds and Hower (1970). A representative structural formula of the exchanged smectites derived from the chemical composition is  $(Si_{7.76} Al_{0.24})(Al_{0.93} Fe_{0.39} Mg_{0.68})Na_{0.62}K_{0.2}O_{22}$ . The CEC and Brunauer Emmet Teller (BET) surface area of the sample are  $80.0 \text{ meq/g}_{\text{clay}}$  and  $94.93 \text{ m}^2/\text{g}_{\text{clay}}$ , respectively (*e.g.* Gammoudi *et al.*, 2012).

The HDPy<sup>+</sup>-modified clay (EP-HDPy<sub>3CEC</sub>) was prepared according to the batch method described in previous reports (Gamoudi *et al.*, 2012). The molar ratio of surfactant HDPy<sup>+</sup> to the CEC was 3.0:1.0 for the EP-Na clay.

### Characterization of adsorbents

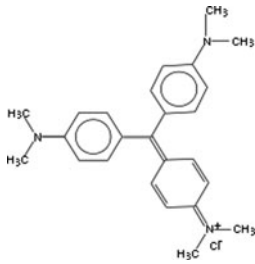
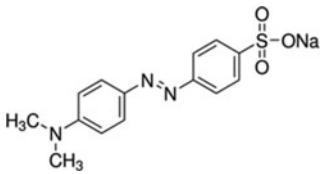
X-ray diffraction analysis was performed using a PANalytical X'Pert HighScore Plus diffractometer with monochromated  $Cu-K\alpha_1$  radiation (30 mA and 40 kV) over the range  $3-20^\circ 2\theta$  at a scanning speed of  $2^\circ 2\theta \text{ min}^{-1}$ .

### Fourier transform infrared spectroscopy (FTIR).

Infrared spectra were obtained using a Perkin-Elmer FTIR (model 783) spectrometer with a smart endurance single-bounce diamond ATR cell. Spectra over the  $400-4000 \text{ cm}^{-1}$  range were obtained by the co-addition of 64 scans with a resolution of  $4 \text{ cm}^{-1}$  and a mirror velocity of  $0.632 \text{ cm s}^{-1}$ . KBr pellets were prepared by mixing clay with KBr at 5 wt.% concentration.

*Surface-charge density,  $\sigma_H$ .* The surface-charge density was determined by potentiometric acid-base titration using NaCl as a background electrolyte at

TABLE 1. Physicochemical characteristics of the dyes used.

Name	Crystal violet	Methyl orange
Chemical structure		
Nature	Cationic	Anionic
Formula	C <sub>25</sub> H <sub>30</sub> N <sub>3</sub> Cl	C <sub>14</sub> H <sub>14</sub> N <sub>3</sub> O <sub>3</sub> SNa
Molar mass (g/mol)	407.97	327.33
Solubility (g/L)	4.2	5.2
λ <sub>max</sub> (nm)	584	464

constant ionic strength (0.1 M). The pH was measured using a Corning pH glass combination electrode which was calibrated with buffer solutions at pH = 4 and pH = 9.18. The  $\sigma_H$  was calculated as the difference between the total amount of H<sup>+</sup> or OH<sup>-</sup> added to the dispersion and that required to bring a blank solution with the same NaCl concentration to the same pH (Schroth & Sposito, 1997):

$$\sigma_H (\text{mol} \cdot \text{m}^{-2}) = \frac{V}{m} S \left\{ ([H^+]_b - [H^+]_s) - \left( \frac{K_w}{[H^+]_b} - \frac{K_w}{[H^+]_s} \right) \right\} \quad (1)$$

where  $V$  is the volume of the electrolyte solution equilibrated with the clay (mL);  $[H^+]$  is the solution proton concentration;  $K_w$  is the dissociation product of water, subscripts 's' and 'b' refer to the sample and blank solutions, respectively;  $m$  is the mass of sample used (g) and  $S$  is the specific surface area (m<sup>2</sup>/g).

### Adsorption experiments

Batch experiments of 0.1 g of sample (purified or modified clay) with 50 mL of dye solution were used to test dye adsorption. The clay/dye mixtures were shaken at 2700 rpm for a given time (see below). The suspensions were then filtered and analysed using a UV-visible spectrophotometer (Perkin Elmer model LAMBDA 20) at maximum wavelength absorption for each dye. The maximum was 584 and 464 nm for CV

and MO, respectively. The experiments were carried out by varying initial dye concentration, pH solution, contact time and temperature. The dye quantities adsorbed by two samples were determined from the mass balance equation (equation 2):

$$Q_{\text{ads}} (\text{mg/g}) = \frac{(C_0 - C_{\text{eq}}) \times V_s}{m} \quad (2)$$

Where  $C_0$  and  $C_{\text{eq}}$  are the initial concentration and equilibrium concentration of dye solution (g/L) respectively;  $V_s$  the volume of dye solution (mL) and  $m$  is the amount of clay used (g).

**Effect of pH solution.** To test the effect of solution pH on dye adsorption, the experiments were carried out by adjusting the initial pH to 3.0, 5.0, 7.0, 9.0 and 11.0 using 0.1 M HCl and NaOH solutions with a pH-meter, at initial dye concentration of 200 mg/L, temperature of 298 K and contact time of 2 h.

**Effect of contact time.** The effect of time on adsorption was investigated by varying the time from 10 min to 6 h at 293 K for an initial dye concentration of 200 mg/L.

**Effect of initial dye concentration.** For two samples (purified or modified clay), adsorption equilibrium studies were performed by adding 0.1 g of sample to 50 mL of various dye solutions (10–500 mg/L) in stoppered bottles. The flasks were stirred for 24 h using a mechanical shaker at 2700 rpm.

*Effect of temperature.* The effect of temperature on dye adsorption was investigated at various temperatures (293–323 K) at an initial dye concentration of 200 mg/L and contact time of 2 h.

### Theoretical considerations

*Adsorption kinetics.* The mechanism of adsorption was investigated using pseudo-first order, pseudo-second order, intra-particle diffusion and Elovich kinetic models to fit the kinetic experimental data. The pseudo-first order kinetics equation may describe the initial phase in the adsorption process but with the progressive adsorption, the data may deviate from the fitting curve. The pseudo-second order equation agrees with chemisorption as the rate-control mechanism. According to the intraparticle diffusion model, several mechanisms are involved and adsorption may consist of three steps: external surface adsorption, intra-particle diffusion which is the rate-limiting step, and the final equilibrium which is very fast. The Elovich equation was used to describe the rate of adsorption that decreased exponentially with increase in the amount of adsorbate but did not provide any mechanistic information about the adsorption process (Yan *et al.*, 2015). The linear form of the pseudo-first order (Lagergren, 1898), pseudo-second order (Ho & McKay, 1999) intra-particle diffusion (Weber & Morris, 1963) and Elovich (Chien & Clayton, 1980) kinetic rate equations are given by equations 3–6, respectively:

$$\ln(Q_e - Q_t) = \ln Q_e - k_1 t \quad (3)$$

$$\frac{t}{Q_t} = \frac{1}{k_2 Q_e^2} + \frac{t}{Q_e} \quad (4)$$

$$Q_t = k_3 t^{1/2} + C \quad (5)$$

$$Q_t = \frac{1}{\beta} \ln(\alpha \cdot \beta) + \frac{1}{\beta} \ln(t) \quad (6)$$

where  $Q_t$  (mg/g) is the amount of dye adsorbed at time  $t$  (min),  $Q_e$  (mg/g) is the equilibrium adsorption capacity,  $k_1$  (1/min) is the rate constant of the pseudo-first order equation,  $k_2$  (g/(mg.min)) is the constant rate of the pseudo-second order equation,  $k_3$  (mg/(g.min<sup>1/2</sup>)) and  $C$  (mg/g) are the rate constant and intercept of intra-particle diffusion equation respectively, and  $\alpha$  (mg/g min) and  $\beta$  (g/mg) are the initial adsorption rate and the parameter related to the extent of surface coverage and activation energy of the Elovich equation, respectively.

The adsorption rate constant,  $k_1$ , for the first-order kinetics was determined from the plot of  $\ln(Q_e - Q_t)$  vs.

$t$ . The equilibrium adsorption capacity ( $q_e$ ) and the second-order rate constant,  $k_2$ , may be determined experimentally from the slope and the intercept of plot  $t/q_t$  vs.  $t$ . The plot of  $q_t$  vs.  $t^{1/2}$  yields a straight line passing through the origin in the case of intra-particle diffusion. The initial adsorption rate,  $\alpha$ , and the parameter  $\beta$ , related to the extent of surface coverage and activation energy of the Elovich equation, were determined from the slope and intercept of the graph by plotting  $q_e$  vs.  $\ln(t)$ .

*Adsorption equilibrium isotherm.* The adsorption isotherm is important in terms of establishing the most appropriate correlation for the equilibrium data for the adsorption batch system. The validity of the conclusions made from the isotherm depends on the adequacy of a model to describe a particular situation. Also, a proper mathematical representation of the equilibrium isotherm, which is based on a correct adsorption mechanism, is essential for an effective design of adsorption systems. In the present study, the adsorption data were tested with respect to the Freundlich, Langmuir, Temkin and Dubinin-Radushkevish isotherm models.

*Langmuir isotherm model.* The Langmuir isotherm is commonly applied in the case of a complete, homogenous surface with negligible interaction between adsorbed molecules. The linear equation of the Langmuir model is as follows (Langmuir, 1916):

$$\frac{1}{Q_{ad}} = \frac{1}{q_{max} k_L} \times \frac{1}{C_{eq}} + \frac{1}{q_{max}} \quad (7)$$

Where  $Q_{ad}$  represents the mass of adsorbed ions per unit of adsorbent (mg/g),  $q_{max}$  is the maximum adsorption capacity corresponding to monolayer coverage;  $k_L$  is the equilibrium constant related to the energy of adsorption and  $C_{eq}$  is the equilibrium concentration of the solution (mg/L).

The essential characteristics of the Langmuir isotherm may be expressed by means of a dimensionless constant,  $R_L$ , known as the equilibrium parameter or separation factor.  $R_L$  may be calculated using the following equation (8):

$$R_L = \frac{1}{\sqrt{1 + k_L \times C_0}} \quad (8)$$

where  $C_0$  (mg/L) is the initial concentration of the dye.  $R_L$  values  $>1$  indicate unfavourable adsorption;  $R_L = 0$  indicates irreversible sorption;  $R_L = 1$  denotes

linear adsorption and  $0 < R_L < 1$  suggests favourable sorption (Robati *et al.*, 2016).

**Freundlich isotherm model.** The Freundlich model is characteristic of heterogeneous surfaces. The Freundlich equation may be represented by the following, linear equation (Freundlich, 1906):

$$\log Q_{ad} = \log k_f + \frac{1}{n} \times \log C_{eq} \quad (9)$$

where  $Q_{ad}$  and  $n$  represent adsorption capacity and intensity, respectively and  $k_f$  is a constant indicative of the adsorption efficiency. The magnitude of  $n$  is indicative of the favourability of adsorption. Values of  $1/n$  of  $<1$  indicate normal adsorption; otherwise, it is indicative of cooperative adsorption. For all examples studied,  $1/n$  was  $<1$  suggesting that adsorption is favourable at high concentrations but less effective at lower concentrations.

**Temkin isotherm model.** Adsorbate–adsorbate interactions are best accounted for by the Temkin isotherm which assumes that the heat of adsorption decreases linearly with coverage due to adsorbate-adsorbate interactions.

The Temkin model is represented in equation 10 (Temkin, 1940):

$$Q_{ad} = B \ln A_T + B \ln C_{eq} \quad (10)$$

where  $B = \frac{R \cdot T}{b_T}$ ;  $b_T$  is the Temkin constant related to adsorption heat,  $R$  is the gas constant,  $T$  is temperature (K) and  $A_T$  is the Temkin parameter related to the equilibrium binding energy.

**Dubinin–Radushkevich isotherm model.** The Dubinin–Radushkevich isotherm is used to estimate the characteristic porosity and the apparent free energy of adsorption. It is useful for determining the nature of adsorption processes whether physical or chemical. The linear form is given in equation 11 (Dubinin & Radushkevich, 1947)

$$\ln Q_{ad} = \ln q_s - k_{ad} \varepsilon^2 \quad (11)$$

where  $q_s$  is the theoretical isotherm saturation capacity (mg/g),  $k_{ad}$  is the activity coefficient related to adsorption mean free energy ( $\text{mol}^2/\text{J}^2$ ) and  $\varepsilon$  is the Polanyi potential given by equation 12:

$$\varepsilon = RT \ln \left( 1 + \frac{1}{C_{eq}} \right) \quad (12)$$

The mean free energy of adsorption ( $E$ , kJ/mol) may be determined using equation 13:

$$E = \frac{1}{\sqrt{2K_{ad}}} \quad (13)$$

This energy gives information about chemical or physical adsorption. For  $8 < E < 16$  kJ/mol, the adsorption is chemical, whereas for  $E < 8$  kJ/mol, the adsorption is physical (Muthukumar *et al.*, 2016).

**Thermodynamic parameters.** The thermodynamic parameters of adsorption,  $\Delta^\circ H$  (kJ  $\text{mol}^{-1}$ ),  $\Delta^\circ S$  (kJ  $\text{mol}^{-1} \text{K}^{-1}$ ) and  $\Delta^\circ G$  (kJ  $\text{mol}^{-1}$ ) might be evaluated using equations 13 and 14 (Freitas *et al.*, 2007):

$$\Delta^\circ G = -RT \ln K_d \quad (14)$$

$$\Delta^\circ G = \Delta^\circ H - T \Delta^\circ S \quad (15)$$

Equations 13 and 14 may be expressed as:

$$\ln K_d = \frac{\Delta^\circ S}{R} - \frac{\Delta^\circ H}{RT} \quad (16)$$

where  $K_d$  is the distribution coefficient of the adsorbate ( $=Q_{ad}/C_e$ ),  $Q_e$  is the amount of adsorbate at equilibrium (mg/kg),  $C_e$  is the equilibrium concentration (mg/L),  $T$  is the absolute temperature (K) and  $R$  is the gas constant =  $8.314 \times 10^{-3}$  kJ  $\text{K}^{-1} \text{mol}^{-1}$ . The plot of  $\ln K_d$  vs.  $\frac{1}{T}$  is linear with the slope and the intercept yielding values of  $\Delta^\circ H$  and  $\Delta^\circ S$ . All these relations are valid when the enthalpy change remains constant in the temperature range studied.

## RESULTS AND DISCUSSION

### Characterization of the adsorbents

**X-ray diffraction analysis.** The modification of the EP-Na by cationic surfactants HDPy<sup>+</sup> through incorporation into the interlayer space was monitored through the swelling of the clay (Fig. 1) In all samples the  $d_{001}$  basal spacing shifted towards higher values after addition of the surfactant, indicating successful intercalation of the surfactant within the clay layers. The EP-Na and EP-HDPy<sub>3CEC</sub> displayed  $d_{001}$  basal spacings of 12.36 Å and 43.97 Å, respectively. The TOT layer thickness of smectite is 9.7 Å (He *et al.*, 2007) and the molecular size of HDPy is 23.1 Å for the “nail-body” (Bors *et al.*, 1999) (*i.e.* the non-polar hydrophobic tail and polar hydrophilic head of the surfactant). Thus, the HDPy molecules in the modified clay obtained a paraffin-type bimolecular arrangement.

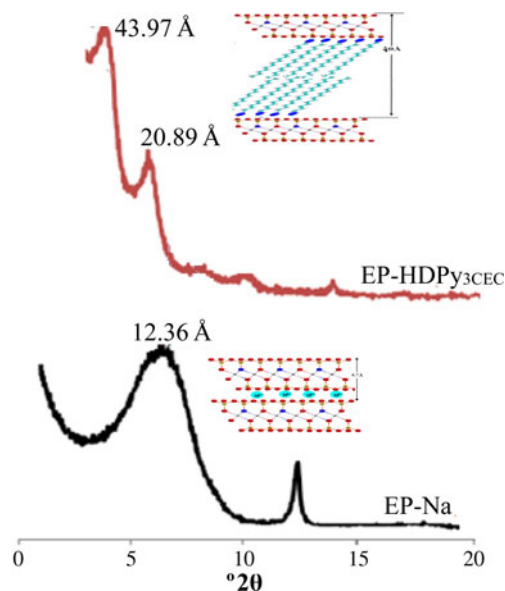


FIG. 1. XRD patterns of purified and modified clays.

**Infrared spectroscopy.** The FTIR spectra of the HDPy surfactant molecules, the purified (EP-Na) and the organo-clay EP-HDPy<sub>3</sub>CEC samples are shown in Fig. 2. The spectra of the HDPy-modified clay are characterized by a N–H stretching band at  $\nu = 3452 \text{ cm}^{-1}$ , pyridine vibrations at  $1639 \text{ cm}^{-1}$ , C–H stretching bands of CH<sub>2</sub> at  $2920$  and  $2850 \text{ cm}^{-1}$  and finally, aromatic C=C vibrations at  $1473$  and  $1373 \text{ cm}^{-1}$  (Bors *et al.*, 2001). The IR spectrum of the organoclay also contains absorption bands at  $\nu = 3620 \text{ cm}^{-1}$  corresponding to

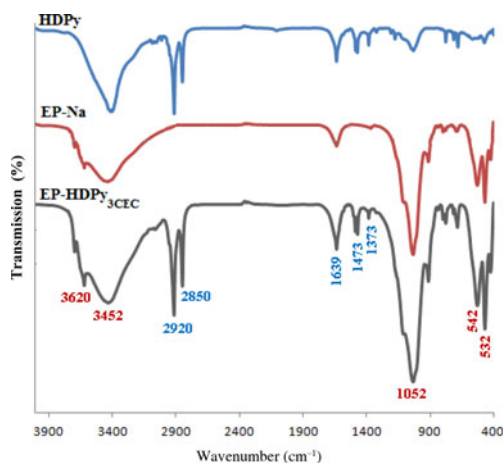


FIG. 2. FTIR spectra of HDPy surfactant, purified and modified clays.

Al–OH–Al stretching vibrations and characteristic Si–O–Si vibrations at  $1052 \text{ cm}^{-1}$ . Antisymmetric and symmetric Si–O bending modes are also present at  $542$  and  $532 \text{ cm}^{-1}$ .

**Surface charge density.** The surface proton density  $\sigma_{\text{H}}$  data vs. the pH of the clay and organoclay dispersed in  $0.1 \text{ M NaCl}$  in the pH range  $2.5$  to  $11$  are shown in Fig. 3. The titration curves were similar in shape for the range of pH used and comparable to those published in the literature (Hamdi & Srasra, 2014). For the purified clay, the titration curves have two branches:  $\sigma_{\text{H}}$  is positive in the acidic pH range due to the protonation of surface functional (Al–OH and Si–OH) groups and negative in the alkaline range due to deprotonation. The organoclay has a surface charge density which is greater than that of the purified clay, which was produced by protonation and deprotonation of surfactant-hydroxyl surface complexes formed at variable-charge hydroxyl groups at the edges of the clay (Hamdi & Srasra, 2014). The purified clay has a point of zero charge (PZC) of  $6.8$ . After modification by HDPy equivalent to  $3.0 \text{ CEC}$  the PZC shifted to  $7.8$  in agreement with similar studies (Ma *et al.*, 2011; Hamdi & Srasra, 2014).

### Removal of dyes

**Effect of pH.** The pH of the solution is a vital factor in terms of controlling the capacity and mechanism of adsorption. It influences the surface charge of the adsorbent, the solubility of dyes (Subbaiah *et al.*, 2016) the dissociation of functional groups on the active sites of the adsorbent as well as the structure of the dye (Li *et al.*, 2016a). The effect of pH on removal of CV and MO by the EP-Na and EP-HDPy<sub>3</sub>CEC adsorbents is illustrated in Fig. 4.

For CV dye, which has a stable chemical structure, CV<sup>+</sup>, in the pH range  $3$ – $11$  (Adams & Rosenstein, 1914), the increase in pH boosts the adsorption onto two clays from a value of  $59.5 \text{ mg/g}$  at pH  $3.0$  to  $>99.95 \text{ mg/g}$  at pH  $7.0$  for EP-Na and from  $24.6 \text{ mg/g}$  at pH  $3.0$  to  $51.2 \text{ mg/g}$  at pH  $8.0$  for EP-HDPy<sub>3</sub>CEC (Fig. 4a). Earlier works reported that cationic dye sorption increases with increase in pH (Monash & Pugazhenthii, 2010; Sarma *et al.*, 2016). With increasing pH, the protonized surface groups ( $\equiv\text{S-OH}_2^+$ ) of EP-Na (PZC =  $6.8$ ), hydroxyl and carboxylate groups on EP-HDPy<sub>3</sub>CEC (PZC =  $7.8$ ) would deprotonize gradually. The number of negatively charged adsorption sites increased and the surface charge on the beads became negative, which enhanced the electrostatic

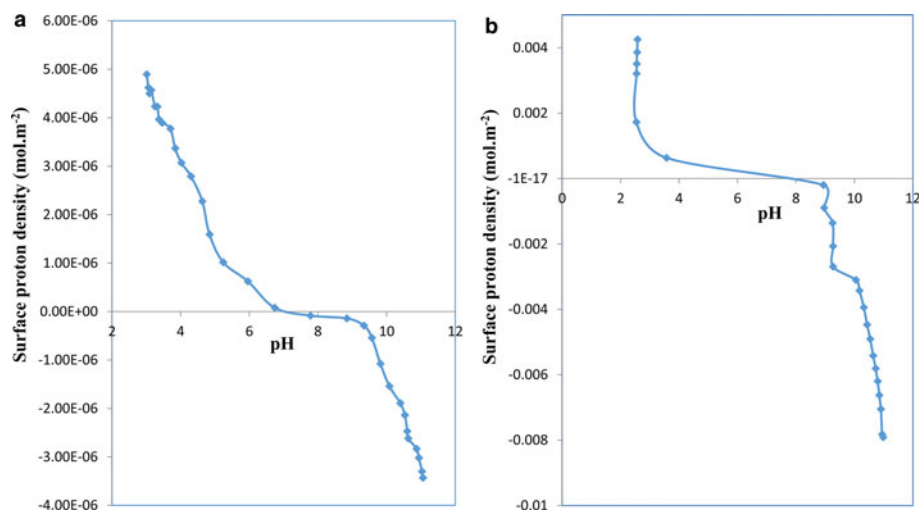


FIG. 3. Potentiometric titration curves vs. pH at ionic strength of 0.1 M and at 279 K: (a) EP-Na and (b) EP-HDPY<sub>3</sub>CEC.

interaction between the cationic dye CV and the adsorbents. The large adsorption capacity of EP-Na was due to the strong electrostatic interaction between the permanent negative charge ( $CEC = 80.0 \text{ meq/g}_{\text{clay}}$ )

and dye cations. In contrast, EP-HDPY<sub>3</sub>CEC contained fewer adsorption sites. Only variable surface charge was presented. Minimum removal of CV was found for  $\text{pH} = 3$ , probably due to the presence of excess  $\text{H}^+$  ions competing with the cation groups on the dye for adsorption sites.

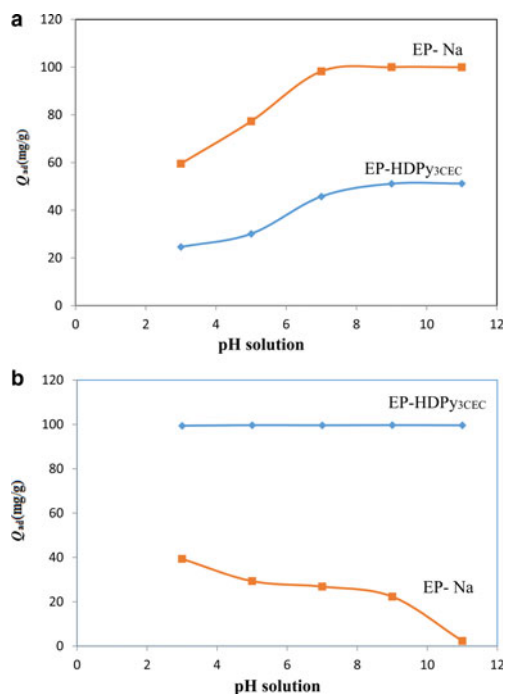


FIG. 4. Effect of pH solution on the sorption of dyes onto purified and modified clays: (a) the cationic dye Crystal Violet; and (b) the anionic dye Methyl Orange.

The MO dye has two chemical structures, the chromophores of which are naphthoquinone, depending on the pH of the solution. The  $\text{pK}_a$  value of MO is 3.37, which means that it is an anion when the solution pH is greater than its  $\text{pK}_a$  value due to the deprotonation of the ammonium ion, MO, from the azonium ion  $\text{MO}^-$  (Tawarah & Abu-Shamleh, 1991). The adsorption of an anionic dye, MO, on EP-HDPY<sub>3</sub>CEC was pH-independent over the pH range 3–11 (Fig. 4b), because of the hydrophobic interaction of the carbon chain of HDPY with the sulfonate groups of the dyes. Similarly, the pH effects on adsorption of anionic dyes on the modified clays were also minimal (Ozan *et al.*, 2004; Baskaralingam *et al.*, 2006). However, an increase in the solution pH from 3 to 11 decreased the MO removal by EP-Na substantially from  $q_{\text{ads}}(\text{MO}) = 39.32 \text{ mg/g}$  to  $q_{\text{ads}}(\text{MO}) = 2.34 \text{ mg/g}$ . At a lower pH value, the electrostatic attraction between the anionic adsorbents and the positively charged adsorption sites increased. As the pH of the system increased, the number of positively charged sites decreased, and the overall surface charge on the surface of EP-Na clay became negative, which reduced the adsorption of anionic molecules.

*Adsorption kinetics.* Equilibrium time is one of the most important parameters affecting the design of

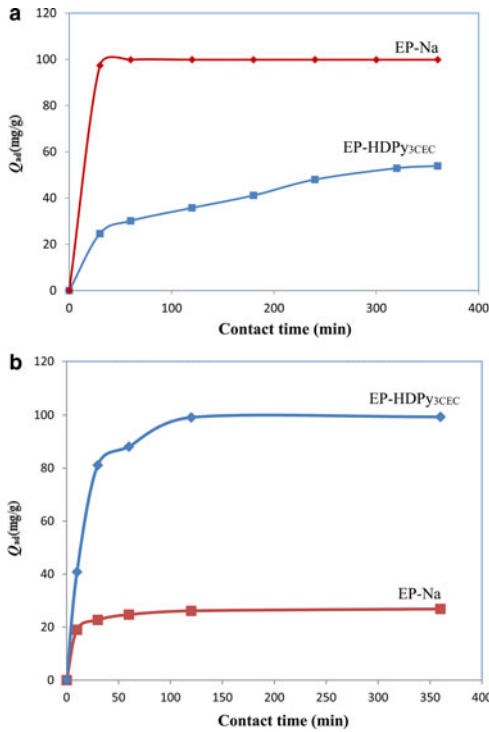


FIG. 5. Effect of contact time on the sorption of dyes onto purified and modified smectites: (a) the cationic dye Crystal Violet; and (b) the anionic dye Methyl Orange.

wastewater-treatment systems. The effect of contact time on the adsorption of CV and MO dyes onto EP-Na and EP-HDPy<sub>3</sub>CEC clays at an initial solution concentration of 200 mg/L is shown in Fig. 5. The adsorption process of MO by two clays was relatively fast, and the adsorption reached equilibrium in <120 min. The adsorption of CV by EP-Na was quick, reaching equilibrium after 60 min but the adsorption of CV by EP-HDPy<sub>3</sub>CEC was much slower, reaching equilibrium after 320 min. These results indicate that the adsorption kinetics are very dependent on the dye structure and the properties of the adsorbant (Santos *et al.*, 2016). The equilibrium capacities were 99.84 and 53.87 mg/g for CV and 26.85 and 199.32 mg/g for MO for the two samples.

Pseudo-first order, pseudo-second order, intraparticle diffusion and Elovich kinetic models were used to evaluate the adsorption kinetics. The estimated kinetic parameters and correlation coefficient ( $R^2$ ) of the four models are summarized in Table 2. For the pseudo-first order model, the  $R^2$  varied from 0.44 to 0.98 and the equilibrium capacity ( $Q_{e,cal}$ ) derived

TABLE 2. Kinetics parameters for the adsorption of CV and MO dyes onto purified and modified clays.

Sample	Dye	$Q_{e,exp}$ (mg/g)	Pseudo-first order		Pseudo-second order		Model							
			$k_1$ ( $\text{min}^{-1}$ )	$Q_{e,cal}$ (mg/g)	$R^2$	$k_2$ ( $\text{g/mg}\cdot\text{min}$ )	$Q_{e,cal}$ (mg/g)	$R^2$	Intraparticle diffusion					
									Elovich					
									$\alpha$ ( $\text{mg/g}\cdot\text{mi}^2$ )	$\beta$ (g/mg)	$R^2$			
EP-Na	CV	99.84	0.012	35.33	0.443	0.03	100.0	1.00	0.122	97.89	0.425	$2.9 e^3$	1.29	0.563
	MO	26.85	0.021	8.51	0.986	0.002	27.78	1.00	0.434	19.86	0.713	$1.6 e^3$	0.44	0.918
EP-HDPy <sub>3</sub> CEC	CV	53.87	0.007	45.60	0.951	0.006	56.67	0.98	2.308	11.53	0.994	2.418	0.08	0.951
	MO	99.32	0.049	108.79	0.962	$8.36 \cdot 10^{-4}$	105.26	0.998	4.095	46.599	0.671	29.38	0.055	0.860



from the equation was much smaller than the equilibrium experimental capacity ( $Q_{e,exp}$ ) (deviations ranging from 15.35 to 181%). The pseudo-first order kinetic model was not suitable, therefore, for modelling sorption process of MO and CV dyes on the two clays. The pseudo-second order kinetic model yielded better fitting with greater coefficients of determination,  $R^2$  (0.98–1.00), than the other kinetic models (Table 2). Hence, the pseudo-second order kinetics may better describe the uptake of CV and MO onto the clays. In addition, the experimental values ( $Q_{e,exp}$ ) show good agreement with the corresponding values calculated by the pseudo-second order model ( $Q_{e,cal}$ ). Similar results have been observed for the adsorption of acid dyes (AB25, AB93, ATBA, AGYG) onto CTMAB-bentonite (Yan *et al.*, 2015), and in the adsorption of cationic dyes (MB, CV, RB) onto organoclays (Anirudhan & Ramachandran, 2015). The adsorption of dyes may be due to electrostatic attraction between the charged surface and charged dye molecules, in conjunction with the chemical characteristics of the clays and dyes molecules (Keyhanian *et al.*, 2011; Muthukumar *et al.*, 2016). The relatively large values of  $k_2$  indicate that the adsorption process is very fast and might reach adsorption equilibrium in a short time (Li *et al.*, 2016a).

On the other hand, the intra-particle diffusion model does not model the adsorption of dyes onto clays as it has large intercept values (97.87–154.1) and the curve does not pass through the origin (Zhang *et al.*, 2014; Muthukumar *et al.*, 2016). Hence, intra-particle diffusion does not seem to control the adsorption of the dyes (Yan *et al.*, 2015). Only the adsorption of cationic dye CV might have been controlled by an intra-particle diffusion mechanism ( $R^2 = 0.994$ ;  $C = 11.53$  mg/g).

**Adsorption isotherms.** The adsorption isotherms for the two dyes are shown in Fig. 6. The amounts of CV and MO adsorbed increased with increasing initial concentrations, until plateaus were reached. This increasing adsorption is because the initial dye concentration acts as a driving force to overcome the mass-transfer resistance for dye transport and fosters the interaction between the adsorbent and dye molecules. However, due to saturation of the active adsorption sites on the material surface at higher dye concentrations, the adsorption capacity declined for the two dyes (Kuppusamy *et al.*, 2016). The adsorption isotherms were H- and S-type for the CV and MO dyes, respectively, according to the Giles classification (Giles *et al.*, 1960). Different adsorption capacities

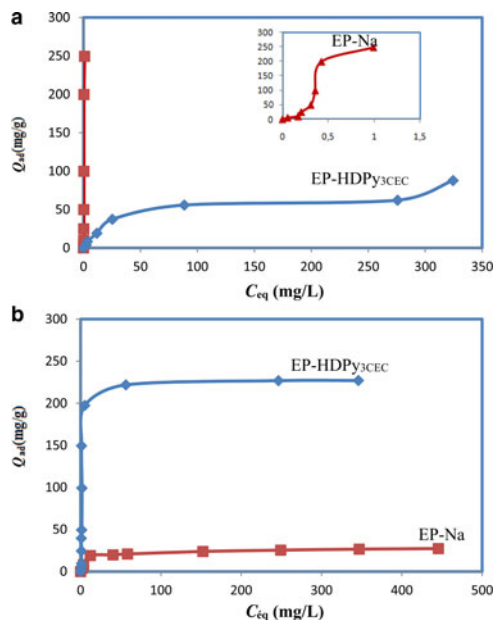


FIG. 6. Retention of dyes by different samples: (a) the cationic dye Crystal Violet; and (b) the anionic dye Methyl Orange.

were observed, suggesting different retention mechanisms of cationic and anionic dyes on the samples.

In order to interpret the adsorption process, Langmuir, Freundlich, Temkin and Dubinin-Radushkevish isotherm models were applied. The adsorption isotherm constants are listed in Table 3.

**Langmuir isotherm model.** The Langmuir model described effectively the sorption data ( $R^2 > 0.99$ ); exceptional removal of MO by EP-HDPy<sub>3</sub>CEC was observed. The maximum monolayer adsorption capacities ( $q_{max}$ ) were estimated as 263.15 and 65.78, respectively, for CV by two clays and 26.45 mg/g for MO by EP-Na, values which are in accord with the experimental data: 249.50 mg/g, 62.78 mg/g and 27.26 mg/g. The large Langmuir equilibrium coefficient,  $K_L$ , obtained (Table 3) suggested the favourable formation of the dye–clay mineral adsorption complex (Sarma *et al.*, 2016). Comparison of the adsorption capacity of the Tunisian clays (purified or modified) with those of various adsorbents from previous studies showed that the purified clay might potentially be used in the removal of the CV dye from aqueous solution and that the modified clay was an effective material in the removal of the MO dye (Table 4). The calculated  $R_L$  values for the dyes were  $0 < R_L < 1$  (Table 3),

TABLE 3. Estimated constants of Langmuir, Freundlich, Temkin and Dubinin-Radushkevich isotherms for CV and MO adsorption by clays.

Sample	Dye	Model													
		Langmuir				Freundlich				Temkin				Dubinin–Radushkevich	
	$q_{\max}$ (mg/g)	$k_L$ (L/mg)	$R^2$	$R_L$	$1/n$	$k_F$ (mg <sup>1/n</sup> /g.L <sup>1/n</sup> )	$R^2$	$A_T$ (L/mg)	$B$	$R^2$	$q_s$ (mg/g)	$k_{ad}$ (mol <sup>2</sup> /J <sup>2</sup> )	$R^2$	$E$ (kJ/mol)	
EP-Na	CV	263.15	0.32	0.99	0.07–0.48	0.46	354.24	0.92	11.73	87.42	0.72	553.9	1.2 <sup>e-5</sup>	0.94	0.204
	MO	26.45	0.12	0.98	0.15–0.74	0.35	21.76	0.89	1.55	4.32	0.97	22.19	1.9 <sup>e-5</sup>	0.95	0.162
EP-HDPy <sub>3CEC</sub>	CV	65.78	0.41	0.99	0.06–0.44	0.51	27.79	0.88	1.7	12.40	0.97	42.94	1.8 <sup>e-5</sup>	0.87	0.166
	MO	277.78	0.24	0.65	0.12–0.54	0.21	78.28	0.56	30.61	26.73	0.71	209.9	4.6 <sup>e-6</sup>	0.91	0.326

suggesting that adsorption of CV and MO by the two clays was favoured.

*Freundlich isotherm model.* The  $R^2$  values for the Freundlich isotherms obtained for the two dyes were <0.9, indicating that the Freundlich model is not suitable for describing the dye adsorption for this study (Table 3).

*Temkin isotherm model.* The calculated values of Temkin constants are listed in Table 3. The model was fitted with  $R^2 = 0.97$  for the retention of CV dye by EP-HDPy<sub>3CEC</sub> clay and MO dye by EP-Na clay. The results assumed also that adsorption is characterized by uniform distribution of binding energies up to a maximum value (Sarma *et al.*, 2016; Lafi & Hafiane, 2016).

*Dubinin-Radushkevich isotherm model.* The  $q_s$  values and  $k_{ad}$  constants and the mean free energy ( $E$ ) values are listed in Table 3. The small free energy ( $E$ , 0.162–0.326 kJ/mol) values obtained indicate that the mechanism of dye adsorption is physisorption due to electrostatic or Van der Waals attractions.

*Thermodynamics study.* The thermodynamic parameters obtained at various temperatures for dye concentrations of 200 mg/L at natural pH are shown in Table 5. Various behaviours for dye adsorption onto purified and modified clays were observed in the temperature range 293–333 K.

For CV dye, the negative values of overall free energy changes,  $\Delta G^\circ$ , indicate that the adsorption process was spontaneous. The decrease in  $\Delta G^\circ$  with increasing temperature suggests that the adsorption is more favoured at higher temperatures. The positive value of  $\Delta S^\circ$  resulted from the increased randomness due to the adsorption of CV, which suggested good affinity of CV for the two adsorbents and increased randomness at the solid–solution interface during the fixation of CV on the active sites of the clays. The positive value of  $\Delta H^\circ$  indicates that the adsorption was an endothermic process (Tahir & Naseem, 2006; Eren, 2009; Jian-min *et al.*, 2010; Depci *et al.*, 2012).

The interactions between anionic dye, MO and the clay minerals were exothermic, however. Similar results have been reported for raw Moroccan clays, Na-bentonite and DTMA-bentonite, organoclays and modified-coffee waste (Ozan *et al.*, 2004; Elmoubarki *et al.*, 2015; Luo *et al.*, 2015; Lafi & Hafiane, 2016). The negative  $\Delta S^\circ$  value suggests a decrease in the randomness at the solid/solution interface during the

TABLE 4. Comparison of adsorption capacities of Tunisian clays with various adsorbents.

Adsorbates	Adsorbents	$Q_{\max}$ (mg/g)	Reference
CV dye	Nanocomposite	28.2	Gholami <i>et al.</i> (2016)
	Red mud	60.5	Zhang <i>et al.</i> (2014)
	Activated carbon	67.1	Hamidzadeh <i>et al.</i> (2015)
	Kaolinite	129.8	Chen <i>et al.</i> (2013)
	Raw bentonite	131.0	Eren (2009)
	HDTMA-bentonite	162.5	Anirudhan (2015)
	Iodo-polyurethane	183.6	Moawed <i>et al.</i> (2015)
	Biosorbent	239.2	Lin <i>et al.</i> (2011)
	Grapefruit peel	249.6	Saeed <i>et al.</i> (2010)
	EP-Na	263.1	This study
MO dye	Graphene oxide	16.8	Yan <i>et al.</i> (2016)
	CTAB-coffee waste	58.82	Lafi & Hafiane (2016)
	Silkworm exuvia	72.0	Chen <i>et al.</i> (2011)
	Nanocomposites	72.6	Istratie <i>et al.</i> (2016)
	HDTMA-zeolite	116.0	Xing <i>et al.</i> (2016)
	Activated carbon	122.0	Mokhtari <i>et al.</i> (2016)
	Organobentonite	141.0	Belhouchat <i>et al.</i> (2016)
	Nanocomposite	145.7	Arshadi <i>et al.</i> (2016)
	Modified-MMT	273.6	Luo <i>et al.</i> (2015)
	EP-HDPy <sub>3CEC</sub>	227.0	This study

adsorption of MO. Also, there are no significant changes in the internal structure of the clay minerals following uptake of the dye molecules (Monash & Pugazhenthii, 2009). The negative values of  $\Delta^\circ G$  indicate that the process is feasible and adsorption is thermodynamically spontaneous.

## CONCLUSIONS

Na<sup>+</sup>-purified and HDPy<sup>+</sup>-modified Tunisian clays were investigated for their ability to remove cationic and anionic dyes (CV and MO) from aqueous solutions

(Table 6). Analysis by XRD and FTIR confirmed the intercalation of HDPy<sup>+</sup> in Na<sup>+</sup>-clay. The basal spacing of the HDPy<sup>+</sup>-clay was 43.97 Å corresponding to a paraffin-type bimolecular arrangement.

The Na<sup>+</sup>-clay is an excellent adsorbent for CV and its modified form, HDPy<sup>+</sup>-clay, would be suitable for removing MO from aqueous solutions. Adsorption of CV was favoured at basic pH, whereas, adsorption of MO was favoured at acidic pH. For two dyes, the pseudo-second order kinetic model was adequate for representing the kinetic data and the Langmuir model was adequate at representing the equilibrium data. The

TABLE 5. Thermodynamic parameters for dye adsorption at various temperatures.

Adsorbent	Dye	$\Delta^\circ H$ (kJ.mol <sup>-1</sup> )	$\Delta^\circ S$ (kJ.mol <sup>-1</sup> .K <sup>-1</sup> )	$\Delta^\circ G$ (kJ.mol <sup>-1</sup> )		
				298	313	323
EP-Na	CV	19.63	0.17	-31.03	-35.28	-36.98
	MO	-20.89	-0.03	-10.75	-9.98	-9.56
EP-HDPy <sub>3CEC</sub>	CV	23.74	0.13	-15.00	-18.25	-19.55
	MO	-89.39	-0.21	-26.81	-23.66	-19.46

TABLE 6. Comparative studies.

Adsorbent	Dye	Adsorption kinetics	Equilibrium isotherms	Thermodynamic studies	Mechanism
EP-Na	CV	Second-order was favourable	Langmuir was favourable One type of adsorption site Monolayer adsorption	Endotherm process Chemical sorption	Single mechanism: cationic exchange
	MO	Second-order was favourable	Langmuir was favourable: One type of adsorption site Monolayer adsorption	Exotherm process Physical sorption	Single mechanism: hydrogen interaction
EP-HDPy <sub>3</sub> CEC	CV	Second-order was favourable	Langmuir was favourable One type of adsorption site Monolayer adsorption	Endotherm process	Single mechanism: partitioning between chain surfactants
	MO	Second-order was favourable	Langmuir and Freundlich were not favourable	Exotherm process Physical sorption dominant	Multiple mechanisms: 1 – hydrophobic interaction; 2 – anionic exchange; 3 – hydrogen interaction

maximum adsorption capacities were 249.50 mg/g for CV and 226.8 mg/g for MO. The adsorption was spontaneous, favourable, endothermic in the case of CV dye and exothermic in the case of MO dye. These results suggest that adsorption of the cationic dye by the clays could be by means of chemisorption. A physisorption process is proposed for the adsorption of the anionic dye, however.

## REFERENCES

- Abdel Messih M.F., Ahmed M.A., Soltan A. & Anis S.S. (2017) Facile approach for homogeneous dispersion of metallic silver nanoparticles on the surface of mesoporous titania for photocatalytic degradation of methylene blue and indigo carmine dyes. *Journal of Photochemistry and Photobiology A: Chemistry*, **335**, 40–51.
- Adams E.Q. & Rosenstein L. (1914) The color and ionization of crystal-violet. *Journal of American Chemical Society*, **36**, 1452–1473.
- Anirudhan T.S. & Ramachandran M. (2015) Adsorptive removal of basic dyes from aqueous solutions by surfactant modified bentonite clay (organoclay): Kinetic and competitive adsorption isotherm. *Process Safety and Environmental Protection*, **95**, 215–225.
- Arshadi M., Mousavinia F., Amiri M.J. & Faraji A.R. (2016) Adsorption of methyl orange and salicylic acid on a nano-transition metal composite: Kinetics, thermodynamic and electrochemical studies. *Journal of Colloid and Interface Science*, **483**, 118–131.
- Baskaralingam P., Pulikesi M., Elango D., Ramamurthi V. & Sivanesan S. (2006) Adsorption of acid dye onto organobentonite. *Journal of Hazardous Materials B*, **128**, 138–144.
- Belhouchat N., Zaghouane-Boudiafa H. & Viseras C. (2016) Removal of anionic and cationic dyes from aqueous solution with activated organo-bentonite/sodium alginate encapsulated beads. *Applied Clay Science*, **135**, 9–15.
- Bors J., Dultz St. & Riebe B. (1999) Retention of radionuclides by organophilic bentonites. *Engineering Geology*, **54**, 195–206.
- Bors J., Patzko A. & Dekany I. (2001) Adsorption behavior of radioiodides in hexadecyl-pyridinium-humate complexes. *Applied Clay Science*, **19**, 27–37.
- Bouraada M., Ouali M.S. & Menorval C.L. (2016) Dodecylsulfate and dodecylbenzenesulfonate intercalated hydrotalcites as adsorbent materials for the removal of BBR acid dye from aqueous solutions. *Journal of Saudi Chemical Society*, **20**, 397–404.
- Chen H., Zhao J., Wu J. & Dai G. (2011) Isotherm, thermodynamic, kinetics and adsorption mechanism studies of methyl orange by surfactant modified silkworm exuviae. *Journal of Hazardous Materials*, **192**, 246–254.
- Chen Z., Wang T., Jin X., Chen Z., Mallavarapu M. & Ravendra N. (2013) Multifunctional kaolinite-supported nanoscale zero-valent iron used for the adsorption and degradation of crystal violet in aqueous solution. *Journal of Colloid and Interface Science*, **398**, 59–66.
- Chien S.H. & Clayton W.R. (1980) Application of Elovich equation to the kinetics of phosphate release and sorption in soils. *Soil Science Society of America Journal*, **44**, 265–268.
- Deng L., Shi Z., Peng X. & Zhou S. (2016) Magnetic calcinated cobalt ferrite/magnesium aluminum hydroxide composite for enhanced adsorption of methyl orange. *Journal of Alloys and Compounds*, **688**, 101–112.
- Depci T., Kul Q.Z., Onal Y., Disli E., Alkan S. & Turkmenoglu Z.F. (2012) Adsorption of crystal violet from aqueous solution on activated carbon derived from Gölbaşı lignite. *Physicochemical Problems of Mineral Processing*, **48**, 253–270.
- Dubin M.M. & Radushkevich L.V. (1947) Equation of the characteristic curve of activated charcoal. *Proceedings of the Academy of Sciences of the USSR. Physical Chemical Section*, **55**, 331–333.
- Elmoubarki R., Mahjoubi F.Z., Tounsadi H., Moustadraf J., Abdennouri M., Zouhri A., El Albani A. & Barka N. (2015) Adsorption of textile dyes on raw and decanted Moroccan clays: Kinetics, equilibrium and thermodynamic studies. *Water Resources and Industry*, **9**, 16–29.
- Eren E. (2009) Investigation of a basic dye removal from aqueous solution onto chemically modified Unye bentonite. *Journal of Hazardous Materials*, **16**, 88–93.
- Errais E., Duplaya J., Elhabiri M., Khodja M., Ocampod R., Baltenweck-Guyote R. & Darragi F. (2012) Anionic RR120 dye adsorption onto raw clay: surface properties and adsorption mechanism. *Colloids and Surfaces A*, **403**, 69–78.
- Estevés B.M., Rodrigues C.S.D., Boaventura R.A.R., Maldonado-Hodar F.J. & Madeira L.M. (2016) Coupling of acrylic dyeing wastewater treatment by heterogeneous Fenton oxidation in a continuous stirred tank reactor with biological degradation in a sequential batch reactor. *Journal of Environmental Management*, **166**, 193–203.
- Freitas A.F., Mendes M.F. & Coelho G.L.V. (2007) Thermodynamic study of fatty acids adsorption on different adsorbents. *The Journal of Chemical Thermodynamics*, **39**, 1027–1037.
- Freundlich H.M.F. (1906) Über die Adsorption in Lösungen. *Zeitschrift für Physikalische Chemie*, **57**, 385–470.
- Gamoudi S., Frini-Srasra N. & Srasra E. (2012) Kinetic and equilibrium studies of fluoride sorption onto

- surfactant-modified smectites. *Clay Minerals*, **47**, 429–440.
- Gholami M., Vardini M.T. & Mahdavinia G.R. (2016) Investigation of the effect of magnetic particles on the Crystal Violet adsorption onto a novel nanocomposite based on Carrageenan-g-poly(methacrylic acid). *Carbohydrate Polymers*, **136**, 772–781.
- Gil A., Assis F.C.C., Albeniz S. & Korili S.A. (2011) Removal of dyes from wastewaters by adsorption on pillared clays. *Chemical Engineering Journal*, **168**, 1032–1040.
- Giles C.H., MacEwan T.H., Nakhwa S.N. and Smith D. (1960) 786. Studies in adsorption. Part XI. A system of classification of solution adsorption isotherms, and its use in diagnosis of adsorption mechanisms and in measurement of specific surface areas of solids. *Journal of the Chemical Society*, **0**, 3973–3993.
- Gupta V.K., Carrott P.J.M. & Ribeiro Carrott M.M.L. (2009) Low-cost adsorbents: Growing approach to wastewater treatment – a review. *Reviews in Environmental Science and Technology*, **39**, 783–842.
- Guz L., Curutchet G., Torres Sanchez R.M. & Candal R. (2014) Adsorption of crystal violet on montmorillonite (or iron modified montmorillonite) followed by degradation through Fenton or photo-Fenton type reactions. *Journal of Environmental Chemical Engineering*, **2**, 2344–2351.
- Hamdi N. & Srasra E. (2014) Acid-base properties of organosmectite in aqueous suspension. *Applied Clay Science*, **99**, 1–6.
- Hamidzadeh S., Torabbeigi M. & Shahtaheri S.J. (2015) Removal of crystal violet from water by magnetically modified activated carbon and nanomagnetic iron oxide. *Journal of Environmental Health Science & Engineering*, **13**, 8–14.
- Hassanzadeh-Tabrizi S.A., Motlagh M.M. & Salahshour S. (2016) Synthesis of ZnO/CuO nanocomposite immobilized on  $\gamma$ -Al<sub>2</sub>O<sub>3</sub> and application for removal of methyl orange. *Applied Surface Science*, **384**, 237–243.
- He H., Zhou Q., Frost R.L., Wood B.J., Duong L.V. & Klopogge J.T. (2007) A X-ray photoelectron spectroscopy study of HDTMAB distribution within organoclays. *Spectrochimica Acta Part A*, **66**, 1180–1188.
- Ho Y.S. & McKay G. (1999) Batch lead(II) removal from aqueous solution by peat: equilibrium and kinetics. *Process Safety and Environmental Protection*, **77**, 165–173.
- Ho Y.S., Chiang C.C. & Hsu Y.C. (2001) Sorption kinetics for dye removal from aqueous solution using activated clay. *Journal Separation Science and Technology*, **36**, 2473–88.
- Hu E., Xinbo W., Songmin S., Xiao-ming T., Shou-Xiang J. & Lu G. (2016) Catalytic ozonation of simulated textile dyeing wastewater using mesoporous carbon aerogel supported copper oxide catalyst. *Journal of Cleaner Production*, **112**, 4710–4718.
- Istrate R., Stoia M., Pacurariu C. & Locovei C. (2016) Single and simultaneous adsorption of methyl orange and phenol onto magnetic iron oxide/carbon nanocomposites. *Arabian Journal of Chemistry*. <https://doi.org/10.1016/j.arabjc.2015.12.012>
- Jian-min R., Wu S. & Jin W. (2010) Adsorption of Crystal Violet onto BTEA- and CTMA-bentonite from aqueous solutions. *World Academy of Science, Engineering and Technology*, **41**, 330–335.
- Keyhanian F., Shariati S., Faraji M. & Hesabi M. (2011) Magnetite nanoparticles with surface modification for removal of methyl violet from aqueous solutions. *Arabian Journal of Chemistry*, **9**, S348–S354.
- Kono H. & Kusumoto R. (2015) Removal of anionic dyes in aqueous solution by flocculation with cellulose ampholytes. *Journal of Water Process Engineering*, **7**, 83–93.
- Kuppusamy S., Thavamani P., Megharaj M., Venkateswarlu K. & Lee Y.B. & Naidu R. (2016) Potential of Melaleuca diosmifolia as a novel, non-conventional and low-cost coagulating adsorbent for removing both cationic and anionic dyes. *Journal of Industrial and Engineering Chemistry*, **37**, 198–207.
- Lafi R. & Hafiane A. (2016) Removal of methyl orange (MO) from aqueous solution using cationic surfactants modified coffee waste (MCWs). *Journal of the Taiwan Institute of Chemical Engineers*, **58**, 424–433.
- Lagergren S. (1898) About the theory of so-called adsorption of soluble substances. *Kungliga Svenska Vetenskapsakademiens Handlingar*, **24**, 1–39.
- Langmuir I. (1916) The constitution and fundamental properties of solids and liquids. *Journal of the American Chemical Society*, **38**, 2221–2295.
- Leodopoulos Ch., Doulia D., Gimouhopoulos K. & Triantis T.M. (2012) Single and simultaneous adsorption of methyl orange and humic acid onto bentonite. *Applied Clay Science*, **70**, 84–90.
- Li H., Sun Z., Zhang L., Tian Y., Cui G. & Yan S. (2016a) A cost-effective porous carbon derived from pomelo peel for the removal of methyl orange from aqueous solution. *Colloids and Surfaces A: Physicochemical and Engineering Aspects*, **489**, 191–199.
- Li H., Liu S., Zhao J. & Feng N. (2016b) Removal of reactive dyes from wastewater assisted with kaolin clay by magnesium hydroxide coagulation process. *Colloids and Surfaces A: Physicochemical and Engineering Aspects*, **494**, 222–227.
- Lin Y., He X., Han G., Tian Q. & Hu W. (2011) Removal of Crystal Violet from aqueous solution using powdered mycelia biomass of *Ceriporia lacerata* P2. *Journal of Environmental Sciences*, **23**, 2055–2062
- Ling F., Fang L., Lu Y., Gao J., Wu F., Zhou M. & Hu B. (2016) A novel CoFe layered double hydroxides adsorbent: High adsorption amount for methyl orange

- dye and fast removal of Cr(VI). *Microporous and Mesoporous Materials*, **234**, 230–238.
- Liu M., Chen Q., Lu K., Huang W., Lü Z., Zhou C., Yu S. & Gao C. (2017) High efficient removal of dyes from aqueous solution through nanofiltration using diethanolamine-modified polyamide thin-film composite membrane. *Separation and Purification Technology*, **173**, 135–143.
- Luo Z., Gao M., Ye Y. & Yang S. (2015) Modification of reduced-charge montmorillonites by a series of Gemini surfactants: Characterization and application in methyl orange removal. *Applied Surface Science*, **324**, 807–816.
- Ma J., Cui B., Dai J. & Li D. (2011) Mechanism of adsorption of anionic dye from aqueous solutions onto organobentonite. *Journal of Hazardous Materials*, **186**, 1758–1765.
- Moawed E.A., Abulkibash A.B. & El-Shahat M.F. (2015) Synthesis and characterization of iodo polyurethane foam and its application in removing of aniline blue and crystal violet from laundry wastewater. *Journal of Taibah University for Science*, **9**, 80–88.
- Mokhtari P., Ghaedi M., Dashtian K., Rahimi M.R. & Purkait M.K. (2016) Removal of methyl orange by copper sulfide nanoparticles loaded activated carbon: Kinetic and isotherm investigation. *Journal of Molecular Liquids*, **219**, 299–305.
- Monash P. & Pugazhenth G. (2009) Adsorption of crystal violet dye from aqueous solution using mesoporous materials synthesized at room temperature. *Adsorption*, **15**, 390–405.
- Monash P. & Pugazhenth G. (2010) Removal of Crystal Violet dye from aqueous solution using calcined and uncalcined mixed clay adsorbents. *Separation Science and Technology*, **45**, 94–104.
- Muthukumar C., Sivakumar V.M. & Thirumarimurugan M. (2016) Adsorption isotherms and kinetic studies of crystal violet dye removal from aqueous solution using surfactant modified magnetic nanoadsorbent. *Journal of the Taiwan Institute of Chemical Engineers*, **63**, 354–362.
- Özan S.A., Erdem B. & Özcan A. (2004) Adsorption of Acid Blue 193 from aqueous solutions onto N-bentonite and DTMA-bentonite. *Journal of Colloid and Interface Science*, **280**, 44–54.
- Özcan A.S., Erdem B. & Özcan A. (2005) Adsorption of Acid Blue 193 from aqueous solutions onto BTMA-bentonite. *Colloids and Surfaces: Physicochemical and Engineering Aspects*, **266**, 73–81.
- Pelaez-Cid A.A., Herrera-Gonzalez A.M., Villanueva M. S. & Bautista Hernandez A. (2016) Elimination of textile dyes using activated carbons prepared from vegetable residues and their characterization. *Journal of Environmental Management*, **181**, 269–278.
- Reynolds P.C. & Hower J. (1970) The nature of interlayering in mixed-layer illite-montmorillonites. *Clays and Clay Minerals*, **18**, 25–36.
- Robati D., Mirza B., Rajabi M., Moradi O., Tyagi I., Agarwal S. & Gupta V.K. (2016) Removal of hazardous dyes-BR 12 and methyl orange using graphene oxide as an adsorbent from aqueous phase. *Chemical Engineering Journal*, **284**, 687–697.
- Rodrigues C.S.D., Carabineiro S.A.C., Maldonado-Hódar F.J. & Madeira L.M. (2017) Wet peroxide oxidation of dye-containing wastewaters using nano-sized Au supported on Al<sub>2</sub>O<sub>3</sub>. *Catalysis Today*, **280**, 165–175.
- Ruan X., Chen Y., Chen H., Qian G. & Frost R.L. (2016) Sorption behavior of methyl orange from aqueous solution on organic matter and reduced graphene oxides modified Ni–Cr layered double hydroxides. *Chemical Engineering Journal*, **297**, 295–303.
- Saeed A., Sharif M. & Muhammad I. (2010) Application potential of grapefruit peel as dye sorbent: Kinetics, equilibrium and mechanism of crystal violet adsorption. *Journal of Hazardous Materials*, **179**, 564–572.
- Santos S.C.R., Oliveira A.F.M. & Boaventura R.A.R. (2016) Bentonitic clay as adsorbent for the decolourisation of dyehouse effluents. *Journal of Cleaner Production*, **126**, 667–676.
- Sarma G.K., Gupta S.S. & Bhattacharyya K.G. (2016) Adsorption of crystal violet on raw and acid-treated montmorillonite, K10, in aqueous suspension. *Journal of Environmental Management*, **171**, 1–10.
- Schroth B.L. & Sposito G. (1997) Surface charge properties of kaolinite. *Clay and Clay Minerals*, **45**, 85–91.
- Subbaiah M.V. & Kim D.S. (2016) Adsorption of methyl orange from aqueous solution by aminated pumpkin seed powder: Kinetics, isotherms, and thermodynamic studies. *Ecotoxicology and Environmental Safety*, **128**, 109–117.
- Tahir S.S. & Naseem R. (2006) Removal of a cationic dye from aqueous solutions by adsorption onto bentonite clay. *Chemosphere*, **63**, 1842–1848.
- Tahir H., Hamed U., Sultan M. & Jahanze Q. (2010) Batch adsorption technique for the removal of malachite green and fast green dyes by using montmorillonite clay as adsorbent. *African Journal of Biotechnology*, **8**, 8206–8214.
- Tang L., Cai Y., Yang G., Liu Y., Zeng G., Zhou Y., Li S., Wang J., Zhang S., Fang Y. & He Y. (2014) Cobalt nanoparticles-embedded magnetic ordered mesoporous carbon for highly effective adsorption of rhodamine B. *Applied Surface Science*, **314**, 746–753.
- Tawarah K.M. & Abu-Shamleh H.M. (1991) A spectrophotometric study of the tautomeric and acid base equilibria of methyl orange and methyl yellow in aqueous acidic solutions. *Dyes and Pigments*, **16**, 241–251.
- Temkin M. & Pyzhev V. (1940) Recent modifications to Langmuir isotherms. *Acta Physicochimica USSR*, **12**, 217–225.

- Vasconcelos V.M., Ribeiro F.L., Migliorini F.L., Alves S. A., Steter J.R., Baldan M.R., Ferreira N.G. & Lanza M.R.V. (2015) Electrochemical removal of Reactive Black 5 azo dye using non-commercial boron-doped diamond film anodes. *Electrochimica Acta*, **178**, 484–493.
- Van Olphen H. (1963) *An Introduction to Clay Colloid Chemistry*. Interscience Publishers, New York, London.
- Vimonses V. (2009) Kinetic study and equilibrium isotherm analysis of Congo red adsorption by clay materials. *Chemical Engineering Journal*, **148**, 354–364.
- Weber J.W.J. & Morris J.C. (1963) Kinetics of adsorption on carbon from solution. *Journal of the Sanitary Engineering Division*, **89**, 31–59.
- Xing X., Chang P., Lv G., Jiang W., Jean J., Liao L. & Li Z. (2016) Ionic-liquid-crafted zeolite for the removal of anionic dye methyl orange. *Journal of the Taiwan Institute of Chemical Engineers*, **59**, 237–243.
- Yan L., Qin L., Yu H., Li S., Shan R. & Du B. (2015) Adsorption of acid dyes from aqueous solution by CTMAB modified bentonite: Kinetic and isotherm modeling. *Journal of Molecular Liquids*, **211**, 1074–1081.
- Yan J., Zhu Y., Qiu F., Zhao H., Yang D., Wang J. & Wen W. (2016) Kinetic, isotherm and thermodynamic studies for removal of methyl orange using a novel-cyclodextrin functionalized graphene oxide-isophorone diisocyanate composites. *Chemical Engineering Research and Design*, **106**, 168–177.
- Yeap K.L., Teng T.T., Poh B.T., Morad N. & Lee K.E. (2014) Preparation and characterization of coagulation/flocculation behavior of a novel inorganic-organic hybrid polymer for reactive and disperse dyes removal. *Chemical Engineering Journal*, **243**, 305–314.
- Zhang L., Zhang H., Guo W. & Tian Y. (2014) Removal of malachite green and crystal violet cationic dyes from aqueous solution using activated sintering process red mud. *Applied Clay Science*, **94**, 85–93.